Original Research Article

Enhanced Proton Conductivity and Stability of Sulfonated Polystyrene-Based Nanocomposite Membranes Incorporating MIL-101(Cr) for Fuel Cell Applications

Valiollah Mandanipour[1] * (iD), Gholamreza Karimipour[2] * (iD), Morteza Montazerozohori[2] (iD), Masoumeh Salehi[1,2] (iD)

[1]Department of Applied Chemistry, University of Gonabad, Gonabad, Iran
[2]Department of Chemistry, Yasouj University, Yasouj, Iran

ARTICLE INFO

ABSTRACT

The development of high-performance proton exchange membranes (PEMs) is crucial for improving the efficiency and durability of fuel cells. In this study, sulfonated polystyrene (SPS) was reinforced with different loadings of MIL-101(Cr) (2.5, 5, and 7.5 wt%), a highly porous metal–organic framework (MOF) with a specific surface area of 1,811.06 m^2 g^{-1}, to fabricate nanocomposite membranes via a solution-casting method. The incorporation of MIL-101(Cr) significantly enhanced key physicochemical and electrochemical properties of the membranes. Water uptake increased from 38.2% to 48.6%, while the ion exchange capacity (IEC) reached up to 0.95 meq g^{-1} with increasing MOF content. The composite membranes exhibited excellent oxidative stability, retaining more than 97% of their original weight after exposure to Fenton's reagent at 80 °C. Electrochemical impedance spectroscopy (EIS) revealed that proton conductivity increased with MIL-101(Cr) loading, reaching a maximum value of 0.0914 S cm^{-1} at 80 °C and 60% relative humidity for the membrane containing 7.5 wt% MIL-101(Cr). In addition, methanol permeability remained in the order of 10^{-7} cm^2 s^{-1}, leading to a markedly improved selectivity factor compared to the MOF-free membrane. These results demonstrate that MIL-101(Cr)-based SPS nanocomposite membranes exhibit a well-balanced combination of high proton conductivity, low methanol crossover, and excellent oxidative stability, highlighting their strong potential for application in next-generation proton exchange membrane fuel cells (PEMFCs) and direct methanol fuel cells (DMFCs).

GRAPHICAL ABSTRACT
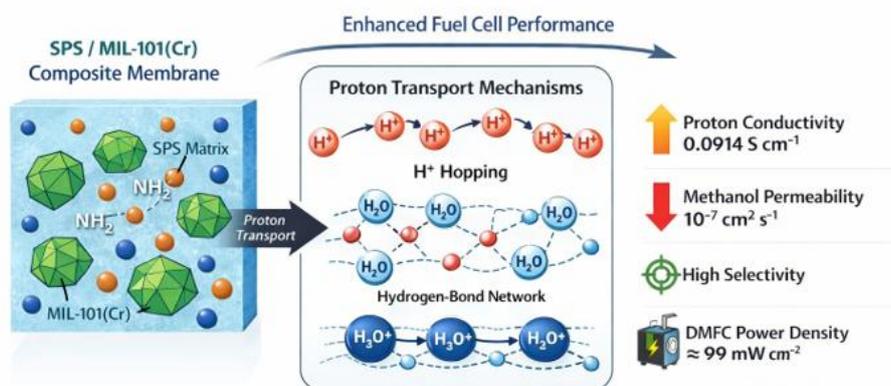
Introduction

Global challenges such as energy shortages and environmental pollution have far-reaching consequences for ecosystems and human health. The rising demand for energy, particularly from fossil fuel sources, has intensified concerns about resource depletion and environmental harm. A significant portion of energy consumption and pollution is attributable to heavy-duty vehicles and passenger cars powered by internal combustion engines. These vehicles emit substantial amounts of carbon dioxide (CO_2) and other hazardous pollutants, thereby exacerbating climate change, air quality deterioration, and environmental degradation. To address these pressing issues, alternative technologies like fuel cells have garnered considerable attention. As highly efficient electrochemical systems, fuel cells facilitate the direct conversion of chemical energy into electrical energy without releasing harmful emissions, positioning them as a promising replacement for conventional combustion engines [1–3].

A fuel cell operates by oxidizing hydrogen at the anode and reducing oxygen at the cathode, with protons moving through the proton exchange membrane (PEM) from the anode to the cathode. This electrochemical process generates electrical energy while water is produced as the only byproduct. The performance of fuel cells is heavily dependent on the proton conductivity of the PEM, which acts as the medium through which protons are transported. Therefore, optimizing the proton conductivity of the PEM is crucial for enhancing fuel cell efficiency and is a key area of research in energy conversion technologies [1–3].

Among the various materials being explored for PEM applications, polymers have garnered significant attention due to their favorable properties, such as high proton conductivity and chemical stability. Perfluorosulfonic acid membranes, such as Nafion, are widely recognized for their excellent conductivity, stability, and durability. However, Nafion membranes face limitations, including high production costs and reduced performance at temperatures exceeding 80 °C. Alternative polymeric materials with improved properties are actively being investigated. One promising candidate is sulfonated polystyrene (SPS), a rigid polymer known for its high thermal and mechanical stability, as well as good chemical resistance. SPS-based membranes have demonstrated considerable proton conductivity; yet; they also suffer from issues such as excessive swelling in hydrated conditions, which reduces mechanical strength. Incorporating nanofillers into the SPS matrix can provide a solution to these problems by enhancing mechanical properties, reducing swelling, and improving overall membrane performance [4–6].

In recent years, metal-organic frameworks (MOFs) have gained significant attention due to their unique combination of organic and inorganic components, which provide highly ordered crystalline structures, large surface areas, and tunable chemical functionality. These features make MOFs excellent candidates for enhancing the performance of PEMs. MIL-101(Cr), a chromium-based MOF, has demonstrated exceptional stability and porosity, making it a promising candidate for use in fuel cells. MIL-101(Cr) possesses functional groups capable of interacting with polymer matrices, and recent studies have shown that its incorporation into polymeric membranes can improve proton conductivity, mechanical strength, and fuel cell performance [7–9].

In this study, the fabrication of nanocomposite membranes was considered by incorporating MIL-101(Cr) as a nanofiller into a SPS matrix via a solution-casting method. MIL-101(Cr) is characterized by its high porosity and abundant functional groups, which are expected to form strong hydrogen-bonding interactions with the polymer matrix. These interactions not only enhance water retention, but also facilitate the

formation of extended hydrogen-bonding networks, providing additional pathways for proton transport. It is hypothesized that MIL-101(Cr) acts as a multifunctional proton-conducting nanofiller, facilitating proton transport through two primary mechanisms: (1) the Grotthuss mechanism, in which protons hop between functional groups within the extended hydrogen-bond network, and (2) the vehicular mechanism, where protons are transported along with water molecules as hydronium carriers. The main objective of this study is to optimize critical membrane properties, including proton conductivity, ion exchange capacity, oxidative and thermal stability, and mechanical strength, while simultaneously minimizing methanol crossover, a significant challenge in fuel cell applications.

To assess the efficiency of the proposed nanocomposite membranes, three distinct compositions with varying concentrations of MIL-101(Cr)-NH$_2$ were synthesized and systematically characterized. Structural and morphological properties were examined through Fourier-transform infrared (FTIR) spectroscopy, and scanning electron microscopy (SEM). Additionally, the porosity of MIL-101(Cr)-NH$_2$ was evaluated using Brunauer–Emmett–Teller (BET) analysis. The findings demonstrated that the incorporation of MIL-101(Cr)-NH$_2$ led to a significant enhancement in proton conductivity, thermal stability, and mechanical strength of the membranes. Under testing conditions of 80 °C and 60% relative humidity, proton conductivities of 0.0785 S cm^{-1}, 0.0897 S cm^{-1}, and 0.0914 S cm^{-1} were recorded for the MM-2.5, MM-5, and MM-7.5 composites, respectively. These values surpass those of many previously reported PEM materials, highlighting the promising potential of MIL-101(Cr)-NH$_2$-based composite membranes for next-generation proton exchange membrane fuel cells (PEMFCs) [10,11].

Overall, this research contributes to the ongoing development of advanced materials for fuel cells and provides insight into the potential of MOF-based nanocomposites for enhancing the efficiency and performance of PEMFCs.

To isolate the contribution of MIL-101(Cr), the performance of MOF-containing membranes was systematically compared with previously reported SPS@PE membranes prepared and tested under identical conditions, enabling a clear assessment of the MOF-induced enhancement.

Experimental

Materials and instrumentation

All chemicals used in this study were of analytical grade and purchased from Merck. SPS was synthesized in-house via the acetyl sulfate method. Chromium (III) nitrate nonahydrate (Cr(NO$_3$)$_3$·9H$_2$O, ≥99%) and terephthalic acid (≥99%) were obtained from Merck and employed to synthesize MIL-101(Cr) through a hydrothermal method. Deionized water was used throughout all preparation and washing steps. Nanocomposite membranes were subsequently fabricated by incorporating different loadings of MIL-101(Cr) into the SPS matrix using a solution-casting technique, followed by controlled drying at ambient temperature.

Characterization techniques included FTIR (AVATAR 370 (Thermo Nicolet, USA)) for functional group identification, and SEM (TESCAN MIRA3 (TESCAN, Czech Republic)) for morphology evaluation. BET (Belsorp mini II (Microtrac Bel Corp, Japan)) surface area analysis was performed to determine porosity. Electrochemical impedance spectroscopy (EIS, Zahner potentiostat/Galvano-stat model PGSTAT) was conducted to measure proton conductivity, while ion exchange capacity (IEC) was assessed via acid-base titration. Thermal stability was analyzed using thermogravimetric analysis (TGA, TGA/DSC 1 (TGA Q50)), and methanol permeability was evaluated through a diffusion cell setup. The membranes' performance in a single-cell fuel system was tested under controlled operating conditions.

Preparation and Characterization

Synthesis of sulfonated polystyrene via acetyl sulfate method

The synthesis of SPS was conducted following a procedure well documented in previous studies reported in the literature [12,13]. Initially, a 2.0 M acetyl sulfate solution (50 mL) was prepared by combining measured quantities of acetic anhydride and dichloromethane under a nitrogen atmosphere. The mixture was cooled to 273 K, and concentrated sulfuric acid (98%) was slowly added. Stirring was continued at room temperature until a homogeneous, transparent solution was formed. To ensure the removal of any residual water, an excess of acetic anhydride was introduced, with additional amounts added if traces of water were detected.

For the sulfonation step, 20.0 g of polystyrene was dissolved in 500 mL of CH_2Cl_2 within a round-bottom flask. The solution was heated to 313 K to achieve complete solubilization and purged with nitrogen gas for 40 minutes. A freshly prepared acetyl sulfate solution was then added to the flask, and the reaction mixture was stirred at 313 K for 2 hours. This resulted in a clear yellow solution, indicative of successful sulfonation. The reaction was terminated by the addition of excess 2-propanol, followed by stirring for 30 minutes and subsequent cooling to room temperature. The final SPS product was then isolated [14].

Preparation of MIL-101(Cr)

1.067 g of terephthalic acid was dissolved in 30 mL of deionized water, and the solution was stirred at room temperature for 15 minutes. Afterward, 2.67 g of chromium nitrate nonahydrate $(Cr(NO_3)3·9H_2O)$ was added to the solution, and stirring was continued for 20 minutes at room temperature. Subsequently, 0.45 mL of hydrofluoric acid (HF) was added to the solution, and the mixture was stirred for 1 hour. The prepared solution was then transferred into an autoclave and heated at 220 °C for 10 hours. The green solid obtained from the reaction was separated, and the precipitate was sequentially washed with ethanol (at 60 °C) and water (at 80 °C) to enhance its purity. The washed precipitate was dried at 100 °C for 2 hours.

The dried precipitate was transferred to 150 mL of ethanol and stirred at 60 °C for 12 hours. It was then filtered, and the precipitate was dried overnight at 60 °C.

The resulting precipitate was placed in 150 mL of water and stirred at 80 °C for 12 hours. It was subsequently filtered and dried overnight at 60 °C.

Finally, the obtained precipitate, identified as MIL-101(Cr), was placed in a vacuum oven at 150 °C and dried overnight to ensure complete dehydration.

Preparation of polymer electrolyte membranes (SPS@PE@MOF)

The polymer electrolyte membrane (PEM) was synthesized using a procedure adapted from previously established methods [15]. Initially, 1.0 g of low-density polyethylene (LDPE) was dissolved in 30 mL of p-xylene, and the resulting mixture was stirred for 2 hours at 373 K and 300 rpm to ensure complete dissolution and uniformity. Following this, 1.0 g of SPS and varying amounts of MIL-101(Cr) (2.5, 5, and 7.5 wt%) were introduced into the solution. p-xylene was used as the solvent to maintain the appropriate viscosity and produce an orange-colored polymer solution.

The polymer solution was then poured onto several glass plates and dried at 318 K for 24 hours to remove the solvent. To ensure thorough solvent evaporation and promote membrane formation, the films were subjected to a vacuum at 348 K for 12 hours. The resulting membrane was denoted as SPS@PE@MOF. The membranes were labeled MM-2.5, MM-5, and MM-7.5, corresponding to the respective weight

percentages of MIL-101(Cr) (2.5%, 5%, and 7.5%) incorporated into the membrane.

Prior to application in a direct methanol fuel cell (DMFC), the membrane was converted to its proton (H⁺) form. This conversion involved boiling the membrane in deionized water for 30 minutes, followed by boiling in 1.0 M sulfuric acid (H_2SO_4) for 24 hours. After acid treatment, the membrane was thoroughly rinsed and reboiled in deionized water until a neutral pH was achieved, ensuring the complete removal of any residual sulfuric acid. The membrane was then stored for subsequent characterization and testing.

Physicochemical properties of the SPS@PE@MOF composite membrane

To assess the performance of the polymer electrolyte membrane (PEM), it is essential to evaluate several key properties, including water uptake, ion exchange capacity, methanol permeability, and selectivity factor.

Water uptake is a critical property that reflects a material's ability to absorb and retain water molecules within its structure. This property plays a significant role across various fields such as materials science, environmental engineering, and biomedical applications. Different materials, including porous solids, polymers, and MOFs, exhibit varying degrees of water uptake, which directly influences their performance in applications such as water purification, drug delivery, and gas separation.

To quantify the water uptake, the membrane was first immersed in deionized water for 24 hours to ensure full saturation. After removing excess surface water, the wet weight (Ww) of the membrane was recorded. The membrane was then dried at 373 K for 2 hours, and the dry weight (Wd) was measured [15,16] using Equation (1).

$$\text{Water uptake (\%)} = \frac{Ww - Wd}{Wd} \times 100 \tag{1}$$

To determine the ion exchange capacity (IEC) of the membranes experimentally, acid-base titration was performed. Initially, the membrane samples were dried until a constant weight was achieved. The samples were then immersed in a saturated NaCl solution for 24 hours to enable proton exchange. Following this, the ion-exchanged solution was titrated with a 0.01 M NaOH solution, with phenolphthalein serving as the indicator. The IEC was calculated using Equation (2).

$$\text{IEC} = \frac{V_{NaOH} \times N_{NaOH}}{W_{dry}} \tag{2}$$

Where,

V_{NaOH}: Volume of NaOH solution used during titration (mL)

N_{NaOH}: Normality of NaOH solution (mol/L)

W_d: Dry weight of the membrane (g)

The oxidative stability of membrane samples, measuring 1.0 × 2.0 × 0.1 cm, was assessed by exposing them to Fenton's reagent. This reagent consisted of 4 ppm ferrous ions (Fe^{2+}) and 3 wt% hydrogen peroxide (H_2O_2) at a temperature of 80 °C. Through an oxidation-reduction reaction, the ferrous ions generate highly reactive hydroxyl radicals, which can break the polymer's chemical bonds.

The initial step involved weighing the membrane samples (W1), followed by immersion in 20 mL of Fenton's reagent for a 24-hour period. After the exposure, the samples were thoroughly rinsed with deionized water. To ensure all moisture was removed, the samples were placed in a vacuum oven at 80 °C for 24 hours. Once dried, the samples were weighed again (W2). The oxidative stability was then calculated using Equation (3):

$$\text{Oxidative stability (\%)} = \frac{W1 - W2}{W1} \times 100 \tag{3}$$

Impedance spectroscopy was performed using a Zahner potentiostat/galvanostat electrochemical workstation (PGSTAT), covering a frequency range from 4 MHz to 1 Hz, with a 5 mV oscillating voltage applied. Proton conductivity measurements at 80 °C were intentionally conducted under 60% relative humidity after allowing the system to equilibrate for one hour to better simulate realistic fuel cell operating

conditions, where fully humidified environments are rarely maintained due to water management limitations and membrane swelling issues. A four-probe method was employed, where two inner platinum (Pt) wires (diameter = 0.2 mm) acted as voltage sensors, while two outer Pt wires (same diameter) were used for AC current injection. Membrane samples, each approximately 3 cm × 1 cm in size, were placed between Teflon blocks and fastened with nylon screws. Prior to measurement, the membranes were conditioned by immersion in a 1.0 M HCl solution for 12 hours, followed by thorough rinsing with deionized water until the pH became neutral. The proton conductivity was determined from the impedance data using Equation (4) [17].

$$\sigma = \frac{L}{RA} \tag{4}$$

where, σ represents the proton conductivity (S/cm), L is the distance between the electrodes (cm), R is the ionic resistance of the membrane obtained from impedance measurements (Ω), and A is the cross-sectional area of the membrane (cm^2).

Methanol permeability was evaluated using a custom-designed two-compartment diffusion cell. The setup consisted of two chambers: the feed chamber (A), which contained a 5 M methanol solution, and the receiving chamber (B), which was filled with deionized water. The receiving chamber was continuously stirred at varying temperatures. A membrane was positioned between the two chambers, and the permeability of the membrane was calculated using Equation (5) [17].

$$P = \frac{1}{CA}\left(\frac{\Delta C_{B(t)}}{\Delta t}\right)\left(\frac{LV_B}{A}\right) \tag{5}$$

where, P denotes the membrane permeability for methanol (cm^2 s^{-1}), CA is the methanol concentration in cell A (mol L^{-1}), $\Delta C_{B(t)}/\Delta t$ represents the rate of change of methanol concentration in cell B (mol L^{-1} s^{-1}), V_B is the volume of each diffusion cell (cm^3), A is the

membrane area (cm^2), and L is the membrane thickness (cm).

The selectivity factor, which is defined as the ratio of proton conductivity to methanol permeability, was calculated using Equation (6) [17].

$$\text{Selectivity} = \frac{\sigma}{P} \tag{6}$$

where, σ represents the proton conductivity (S/cm) and P is the methanol permeability (cm^2 s^{-1}).

Results and Discussion

SEM characterization

In this study, SEM was employed to investigate the morphology and structure of the MOF MIL-101(Cr) both in its pure form and in combination with a composite membrane consisting of polystyrene and polyethylene. The composite membrane was designed with the aim of optimizing proton conductivity while simultaneously preventing methanol crossover, a key factor in enhancing the performance of direct methanol fuel cells (DMFCs). The incorporation of MIL-101(Cr) into the polymer matrix can improve the mechanical strength and thermal stability of the membrane, which are crucial under operational conditions. Additionally, the unique properties of MIL-101(Cr), such as its ability to effectively adsorb CO_2, may play a significant role in managing by-products within the fuel cell environment.

Figure 1A and B present SEM images of MIL-101(Cr), illustrating its morphology and particle size distribution. It should be noted that the pores of MIL-101(Cr) are nanoporous and cannot be directly observed as voids in SEM images. While SEM images do not provide direct evidence of crystallinity, the preservation of the MIL-101(Cr) structure in this work is supported by its characteristic FTIR bands and high BET surface area, which closely match reported values for crystalline MIL-101(Cr) in the literature [18]. The

difference in magnification between the two images allows visualization of the particle size distribution, where finer particles contribute to a higher surface area, potentially influencing adsorption and catalytic activity.

Figure 1C displays the surface morphology of the composite membrane made from polystyrene, polyethylene, and MIL-101(Cr). The surface texture of the membrane can influence both its mechanical properties and its interaction with methanol. As shown in the figure, the MIL-101(Cr) particles are relatively uniformly dispersed within the polymer matrix. This uniform dispersion ensures effective interaction between the MOF particles and the methanol solution. The

membrane surface exhibits significant roughness, which could enhance the contact area and, consequently, improve the fuel cell membrane's performance.

Figure 1D, showing a cross-sectional view of the membrane, provides data on its thickness and layering. As seen in the figure, the membrane thickness (150 μm) is sufficient to prevent direct methanol crossover to the counter electrode while allowing proton transport. The distribution of the various layers of the membrane (polystyrene, polyethylene, and MIL-101(Cr)) is clearly visible. This distribution may affect both the mechanical properties and mass transport characteristics of the membrane.
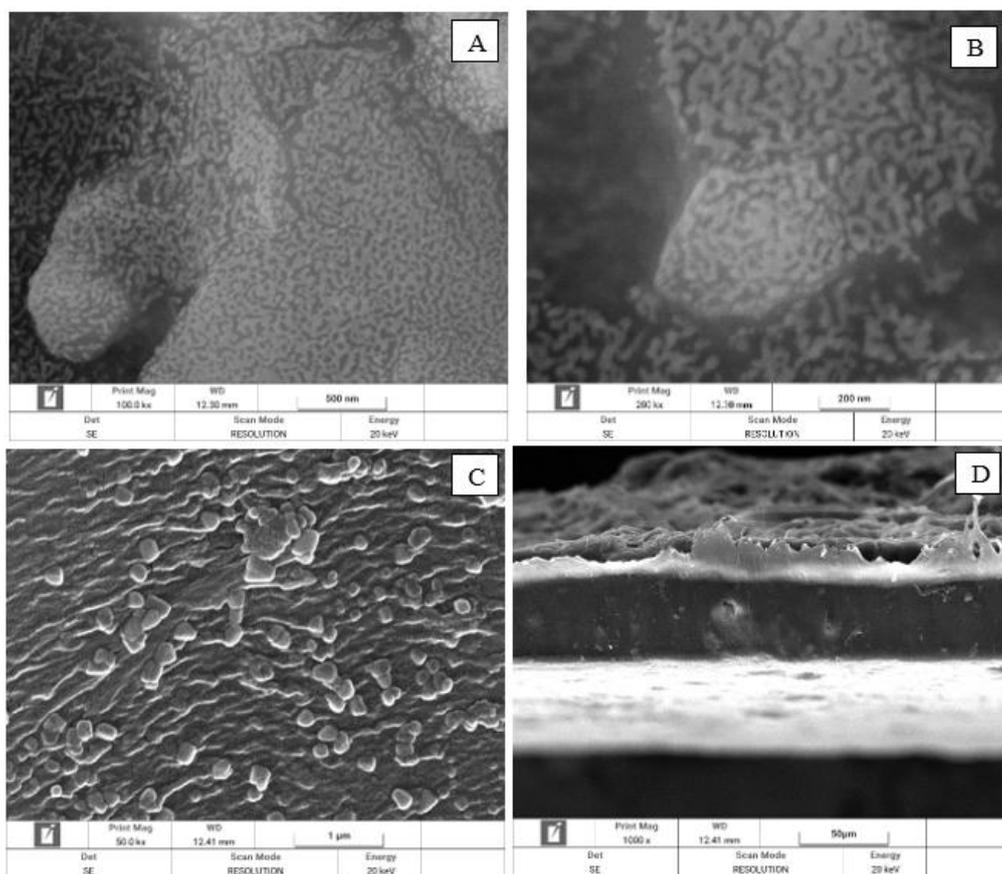

Figure 1. SEM images for (A) and (B) MIL-101(Cr) particles, and (C) surface of SPS@PE@MOF membrane (D) cross-sectional image of the SPS@PE@MOF membrane

BET and BJH analysis of synthesized material

Nitrogen adsorption-desorption experiments were conducted, and the resulting data were analyzed using the BET and Barrett–Joyner–Halenda (BJH) methods to evaluate the surface area and pore characteristics of the synthesized material. BET analysis determined a specific surface area (SSA) of 1,811.06 m²/g. The adsorption-desorption isotherms were classified as type II with a type H3 hysteresis loop, consistent with the IUPAC classification (Figure 2A).

BJH pore size distribution analysis (Figure 2B) demonstrated an average pore diameter of 11.45 nm based on adsorption data, while the cumulative pore volume in the range of 17 Å to 3,000 Å° was 0.0405 cm³/g. The average pore diameter from adsorption, calculated by the BET method, was 12.41 nm, which closely aligns with BJH results. These findings confirm the mesoporous nature of the material and highlight its significant textural properties, making it a promising candidate for applications in catalysis, gas storage, separation processes and membranes requiring mesoporous frameworks.

Although XRD analysis is typically employed to confirm MOF crystallinity, the preservation of MIL-101(Cr) structure in this work is supported by its characteristic FTIR bands and high BET surface area, which closely match reported values for crystalline MIL-101(Cr) in the literature [18].
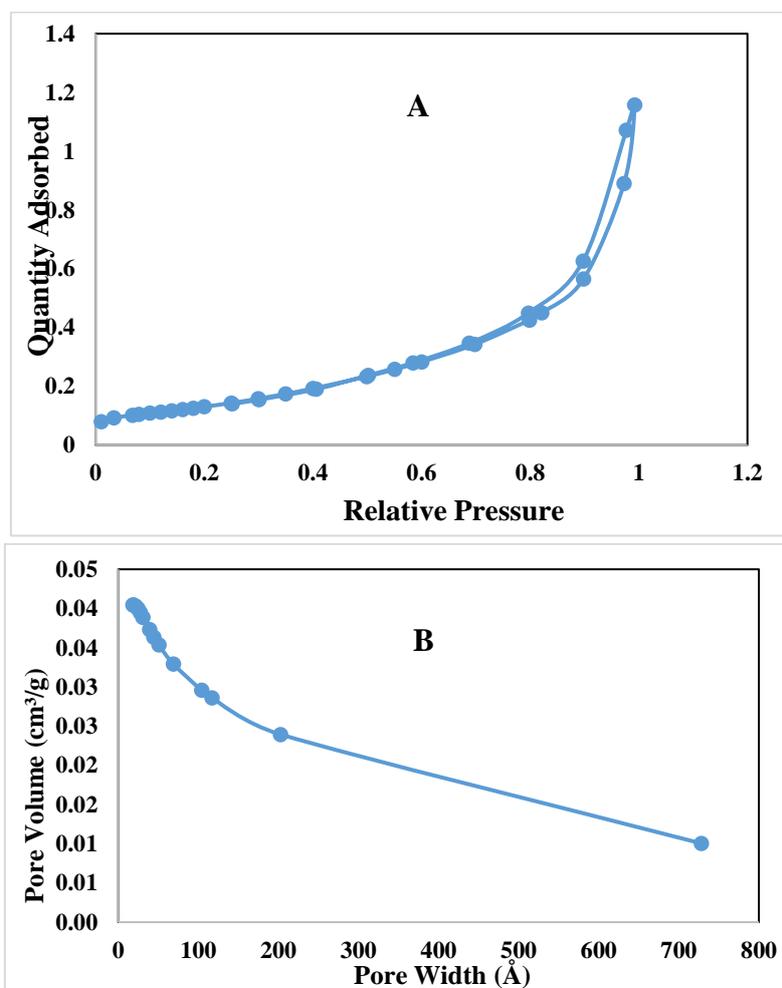

Figure 2. (A) N₂ adsorption/desorption isotherm, and (B) BJH pore size distributions of the MIL-101(Cr)

FTIR analysis of MIL-100(Cr)-NH$_2$ and SPS@PE@MIL-101(Cr)

FTIR is a powerful technique for identifying functional groups and chemical bonds in various materials. Figure 3 displays the FTIR spectra of the synthesized MOF and the composite membrane. For the MIL-101(Cr) MOF, FTIR spectra provide valuable insights into its structure, the presence of functional groups, and its porosity characteristics.

In Figure 3 (A), the peaks observed in the 3,200–3,500 cm^{-1} region correspond to the stretching vibrations of the N–H bond. These peaks confirm the presence of amine (NH$_2$) groups within the material's structure. The broad nature of these peaks is likely due to the formation of hydrogen bonds between amine groups or with other electronegative atoms present in the structure. The peaks in the 1,550–1,650 cm^{-1} region are associated with the bending vibrations of the NH$_2$ group and the stretching vibrations of the C=O bond (if carbonyl groups are present). The presence of these peaks further validates the effective incorporation of amine groups within the material's structure. The peaks in the 1,200–1,400 cm^{-1} region are attributed to the bending vibrations of the CH$_2$ group and the stretching vibrations of the C–N bond. These peaks indicate the presence of organic chains in the material's framework. Finally, the peaks observed below 1,000 cm^{-1} are linked to complex vibrations involving interactions between metal atoms and oxygen. These peaks provide crucial information regarding metal-oxygen bonds within the MOF.

This analysis highlights the structural features and the presence of functional groups in MIL-101(Cr), confirming their role in enhancing the properties of composite membranes.

Figure 3 (B) shows the spectrum corresponding to the SPS@PE@MIL-101(Cr) membrane. As can be seen from the figure, the strong peaks observed in the range of 3,500–3,000 cm^{-1} correspond to the stretching vibrations of O-H and N-H bonds. These peaks indicate the presence of hydroxyl groups (likely from adsorbed water or functional groups) and amine groups in MIL-101(Cr). The peaks within the range of 3,000–2,800 cm^{-1} are associated with the stretching vibrations of C-H bonds in aliphatic groups (from polyethylene) and aromatic groups (from polystyrene). The peaks in the range of 1,640 cm^{-1} are attributed to the stretching vibrations of C=O bonds, while those in the range of 1,500–1,300 cm^{-1} are related to the bending vibrations of N-H bonds in amines and the stretching vibrations of C=C bonds in aromatic rings. These peaks confirm the presence of benzene rings in polystyrene and amine groups in MIL-101(Cr). The weak peaks appearing in the range of 1,400–1,000 cm^{-1} correspond to various vibrations, including C-H bending vibrations and C-O and C-N stretching vibrations. The peak at approximately 1,123 cm^{-1} may be attributed to the stretching vibrations of the S=O bond, indicative of sulfonic acid groups in SPS. Additionally, the peaks below 1,000 cm^{-1} are characteristic of complex vibrations associated with the overall molecular structure.

In conclusion, the FTIR spectrum provides clear evidence that the SPS@PE@MIL-101(Cr) membrane contains multiple functional groups, including hydroxyl, amine, carbonyl, sulfonic acid, and aromatic rings. The presence of these functional groups strongly supports the incorporation of SPS, polyethylene, and the MOF MIL-101(Cr) within the composite structure, confirming its multi-component and functionalized nature.
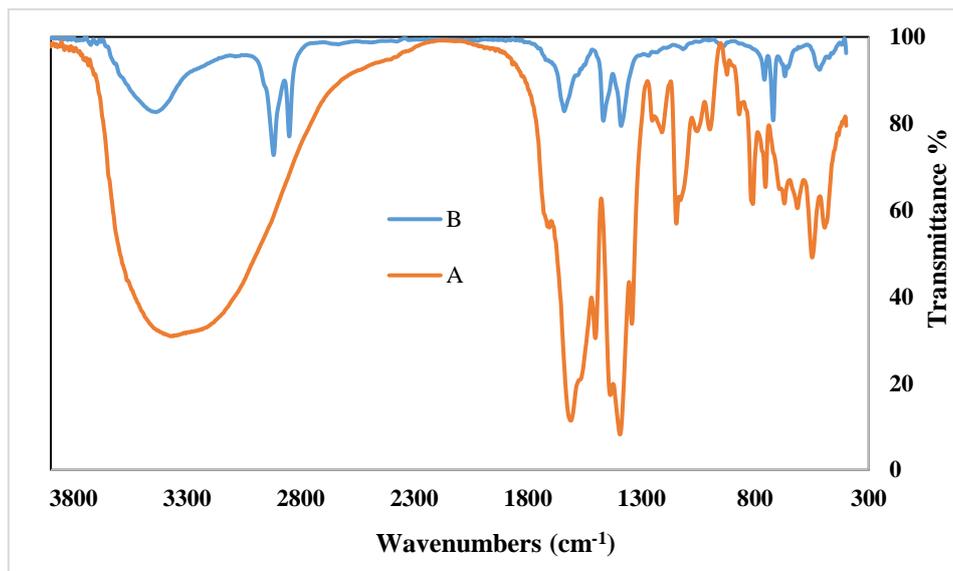
Figure 3. FTIR spectra of (A) MIL-100(Cr)-NH$_2$ particles (B) SPS@PE@MIL-101(Cr) membrane

Water uptake (WU)

The capacity of fuel cell membranes to facilitate proton transport from the anode to the cathode is a fundamental property that directly determines their operational efficiency. Water uptake, as a critical parameter, plays an essential role in enhancing proton conductivity by creating a conducive medium for the mobility of hydrogen ions. An adequate level of water within the membrane promotes the formation of continuous pathways for proton conduction, thereby maximizing proton conductivity. However, excessive water absorption can lead to membrane swelling, which compromises mechanical properties and structural integrity. Such swelling may result in membrane cracking, reduced operational durability, and diminished performance under demanding conditions. Thus, precise control of water uptake is crucial to maintaining an optimal balance between proton conductivity and mechanical stability.

Experimental results on water uptake for synthesized composite membranes were obtained under 100% relative humidity at 25 °C, both in air and in water equilibrated at the same temperature. The water uptake values for the MM-2.5, MM-5, and MM-7.5 membranes were determined to be 38.2%, 47.3%, and 48.6%, respectively (Table 2).

The findings indicate that increasing the content of MOFs within the membrane structure enhances water uptake. This enhancement can be attributed to the high affinity of MOFs for water molecules through the formation of hydrogen bonds, thereby increasing the membrane's water retention capability. Furthermore, the presence of functional groups, such as NH$_2$, on the membrane surface significantly amplifies its water absorption capacity.

Interestingly, the results reveal a nonlinear relationship between MOF content and water uptake. For instance, increasing the MOF content from 2.5 to 5% resulted in an approximate 10% rise in water uptake. However, a further increase from 5 to 7.5% led to only a marginal improvement of about 1%. This reduction in incremental water uptake may stem from excessive MOF loading, which could partially block the internal channels and pores of the membrane, restricting water accessibility.

These observations underscore that while MOF incorporation can substantially enhance water uptake, there exists an optimal MOF concentration. Beyond this threshold, additional MOF loading yields diminishing returns and may even negatively impact water absorption properties due to structural obstruction. This finding highlights the need for careful optimization of MOF content to balance water uptake efficiency with membrane structural performance in practical applications.

Proton conductivity

Membranes employed in direct methanol fuel cells must possess the ability to effectively transfer protons from the anode to the cathode to ensure optimal system performance. Functional groups such as SO_3H, NH_2, and $COOH$ are pivotal in enhancing proton transfer. These groups, through the formation of strong hydrogen bonds with water molecules, enhance the membrane's water absorption capacity. Increased water uptake creates continuous conduction pathways for protons, thereby significantly improving proton conductivity. Furthermore, the presence of these functional groups in the membrane structure not only accelerates proton transfer, but also boosts the thermal and chemical stability of the membrane.

Table 1 illustrates the proton conductivity of composite membranes containing varying concentrations of MIL-101(Cr) at 25 °C and 100% relative humidity, as well as at 80 °C and 60% relative humidity. As anticipated, an increase in the MIL-101(Cr) content, due to a rise in NH_2 groups, enhances proton transfer, thereby improving the membrane's proton conductivity.

The incorporation of MIL-101(Cr) into the polymer matrix, particularly up to a 5 wt% loading, significantly improves proton conductivity. However, further increasing the filler content to 7.5 wt% results in a minimal increase in proton conductivity. This slight enhancement is likely due to the excess MIL-101(Cr) particles exceeding the polymer's pore size, which interferes with their effective distribution within the matrix.

Both temperature and MIL-101(Cr) content have a positive impact on proton conductivity. At higher temperatures, composite membranes exhibit notably improved proton conductivity, with values of 785, 897, and 914 mS cm^{-1} for MM-2.5, MM-5, and MM-7.5, respectively, at 80 °C.

This enhanced proton conductivity can be attributed to the unsaturated metal sites in MIL-101(Cr), which facilitate the formation of hydroxyl groups through hydrolysis. These hydroxyl and NH_2 groups, in turn, promote proton transport via the Grotthuss mechanism. Moreover, increasing the MIL-101(Cr) concentration further expands hydrogen bonding networks, which contributes to an overall improvement in proton conductivity.

Comprehensive performance evaluation of composite membranes for direct methanol fuel cells

The water uptake, ion exchange capacity (IEC), proton conductivity (σ), methanol permeability (P), selectivity (σ/P), and oxidative stability of the

Table 1. Proton conductivity (σ) and relative humidity (RH) of SPS@PE@MOF composite membranes with different amounts of MIL-101(Cr) at 25 and 80 °C

Sample	σ× 10^{-2} (S cm^{-1})	
	25 °C (100% RH)	80 °C (60% RH)
MM-2.5	3.67	7.85
MM-5	4.95	8.97
MM-7.5	5.03	9.14

composite membranes are summarized in Table 2. IEC is a fundamental parameter for evaluating a membrane's ability to facilitate proton transfer from the anode to the cathode in direct methanol fuel cells (DMFCs). This parameter is particularly useful for assessing both the proton conductivity and the presence of proton-exchangeable groups in the membrane. The ion exchange capacity of the synthesized membranes was determined following standardized testing procedures. The results reveal that all composite membranes exhibit significantly high IEC values, indicating their effectiveness in proton transport. These elevated IEC values confirm that the membranes are well-suited to efficiently transfer protons, ensuring their high performance in fuel cell applications. Furthermore, the observed high IEC suggests an efficient proton-exchange mechanism, enhancing the overall ionic conductivity of the membranes.

The proton conductivity of the membrane samples was measured at 25 °C and 100% relative humidity. To prepare the samples, the composite membranes were soaked in water for 24 hours. The results showed that the membranes exhibited considerable proton conductivity, which can be attributed to the presence of functional groups such as $-SO_3H$, $-NH_2$, and $-COOH$ within their structure. These functional groups enhance proton transport by forming hydrogen bonds with water molecules, which increases the membrane's water absorption capacity and, in turn, improves proton conduction within the membrane.

To assess the methanol permeability of the membranes, a series of experiments were performed at room temperature using a 5 M methanol solution. The corresponding methanol permeability values for each membrane are presented in Table 2. The observed trend in methanol permeability across the membranes is as follows: MM-7.5 > MM-5 > MM-2.5.

The results showed that increasing the MIL-101(Cr) content from 2.5 to 7.5% significantly improved water absorption, which, in turn, led to an increase in methanol permeability within the membrane structure. The enhanced water uptake is attributed to the higher concentration of hydrophilic functional groups, which facilitate the absorption of water molecules, thus improving the overall transport of methanol through the membrane.

However, when the MIL-101(Cr) content was increased beyond 5%, the permeability did not show a significant improvement. In fact, further increases in the MIL-101(Cr) loading resulted in the formation of blockages within the membrane's channels and pores. These blockages are believed to hinder the free flow of methanol and water, limiting the membrane's performance. Despite these effects, the overall differences in methanol permeability values among the various membranes were relatively minor, suggesting that an optimal balance of MIL-101(Cr) content is necessary to achieve the best performance in terms of methanol permeability while avoiding the formation of structural obstructions.

For direct methanol fuel cells (DMFCs), the ideal membrane properties include low methanol permeability coupled with high proton conductivity. To assess and enhance the performance of DMFC membranes, the selectivity factor—defined as the ratio of proton conductivity to methanol permeability—plays a crucial role. A higher selectivity factor indicates superior fuel cell performance, as it signifies a membrane's ability to conduct protons efficiently while minimizing methanol crossover, a key factor that influences the efficiency of the fuel cell. This factor is particularly important because methanol crossover can significantly decrease the overall fuel cell efficiency by reducing the availability of methanol at the anode and increasing fuel loss.

Table 2 presents the oxidative stability of the membranes under the influence of Fenton's reagent at 80 °C, a commonly used oxidative agent. The results indicate that the membranes

showed excellent oxidative stability, maintaining more than 97% of their original weight after exposure for one hour. This remarkable stability can be attributed to the robust crosslinking network formed between the MOF functional groups and the SPS-PE polymer matrix. The crosslinking enhances the mechanical integrity and resistance of the membrane to oxidative stress, ensuring that the structure remains intact even under harsh operating conditions. Such stability is critical for the long-term durability and performance of DMFC membranes, as it prevents degradation over time and contributes to the membrane's overall longevity in fuel cell applications. Furthermore, the resistance to oxidative damage indicates the membrane's potential to perform efficiently over extended periods, especially in environments where high temperatures and oxidative agents are present.

All three membranes prepared in this study exhibited superior performance compared to the MOF-free membrane, as summarized in Table 2.

Table 2. Water uptake, ion exchange capacity, proton conductivity, methanol permeability, selectivity, and oxidative stability factor of composite membranes, compared with the corresponding MOF-free membrane

Membrane	WU%	IEC (meq.g^{-1})	$\sigma \times 10^{-2}$ (S.cm^{-1})	P $\times 10^{-7}$ (cm^2.s^{-1})	σ / P $\times 10^4$ (S.s.cm^{-3})	Oxidative stability (Wt %)	Ref.
MM-2.5	38.2	0.93	3.67	8.67	4.23	> 97	This work
MM-5	47.3	0.95	4.95	8.71	5.68	> 97	This work
MM-7.5	48.6	0.95	5.03	8.73	5.76	> 97	This work
SPS@PE	41.67	0.95	2.72	8.92	3.05	> 97	[11]

TGA characterizations

The TGA curves for three different membranes, namely MM-2.5, MM-5, and MM-7.5, are depicted in the diagram. These membranes differ in the amount of MIL-101(Cr) MOF incorporated into their structure. As illustrated in Figure 4, all three membranes exhibit a notable weight loss between 100 °C and 200 °C. This early-stage weight loss is likely attributed to the evaporation of water absorbed within the membrane's matrix and possibly the release of solvents with low boiling points.

At elevated temperatures, specifically in the range of 300 to 500 °C, a more pronounced weight loss occurs for all the membranes. This significant weight reduction is indicative of the thermal degradation of organic components within the membrane, such as polyethylene, polystyrene, and the organic chains of the MOF structure. The data further show that as the MOF content increases from 2.5% in MM-2.5 to 7.5% in MM-7.5, the primary weight loss during thermal decomposition also rises. This suggests that the increased MOF content accelerates the breakdown of the MOF as an organic material at elevated temperatures, contributing to the observed increase in weight loss.

Interestingly, the membrane with the lowest MOF content (MM-2.5) demonstrates greater thermal stability, maintaining its structure up to higher temperatures. This observation implies that increasing the concentration of MOF can reduce the overall thermal stability of the membrane, likely due to the lower thermal resistance of the MOF material compared to the polymer matrix. Furthermore, the weight loss observed above 600 °C for the SPS@PE@MOF membranes is attributed to the complete breakdown of both the polymer matrix and the organic-inorganic hybrid framework of the membrane. This decomposition highlights the

inherent instability of the organic components under extreme thermal conditions, which ultimately affects the durability and long-term

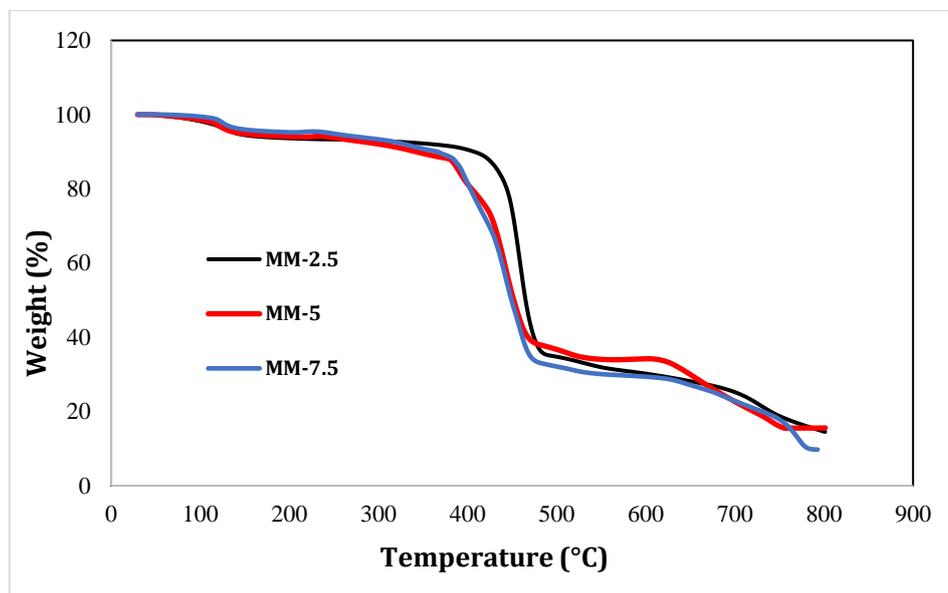performance of the membrane in high-temperature applications.

Figure 4. TGA analysis of the membranes in a temperature range from 30 to 800 °C

Evaluation of the performance of the proposed membranes in single-cell systems

Single-cell tests were performed on composite membranes within the CH_3OH/O_2 system to assess their performance. Figure 5 displays the outcomes of the single-cell tests conducted using a membrane electrode assembly (MEA) composed of three different formulations. These tests were carried out under conditions where oxygen was present on the cathode side and 2 M methanol on the anode side, with the system operating at 80 °C and a flow rate of 1 mL min^{-1}. The findings indicated that the MM-5 and MM-7.5 membranes outperformed the MM-2.5 membrane, achieving a power density of approximately 99.05 mW cm^{-2}. This suggests that altering the membrane composition can have a considerable impact on the performance of the fuel cell.

The MM-2.5 membrane, with a power density of 85.19 mW cm^{-2}, showed comparatively lower performance than the other two membranes. This difference underscores the significant effect of

changes in the membrane's composition and structure on the fuel cell's efficiency. The highest current density, 719.57 mA cm^{-2}, was recorded for the MM-7.5 membrane, highlighting its exceptional ability to facilitate proton transfer and generate electricity. Meanwhile, the MM-2.5 and MM-5 membranes demonstrated current densities of 573.75 mA cm^{-2} and 685.02 mA cm^{-2}, respectively, further reinforcing their strong performance in proton conduction and electricity generation.

One of the key factors that contributed to the enhanced performance of these membranes was the integration of MOFs within their structure. The incorporation of MOFs significantly increased the membrane porosity, which facilitated proton movement. This, in turn, improved the efficiency of the electrochemical reactions occurring within the fuel cell. Additionally, the introduction of NH_2 and SO_3 functional groups within the membrane structure reinforced hydrogen bonding, leading to greater water retention and further enhancing proton transfer. These improvements were

instrumental in boosting the membranes' performance in fuel cells, optimizing the overall functionality of the system.

The trend observed in the increased selectivity of the membranes demonstrated that higher selectivity corresponded with improved performance in open-circuit voltage (OCV). This was mainly attributed to the reduced methanol permeability through the membranes and the enhanced efficiency of proton transfer. In essence, membranes with higher selectivity exhibited superior proton conduction while simultaneously preventing methanol crossover, which played a crucial role in enhancing the overall fuel cell efficiency.

Thus, it can be concluded that the effective integration of MOFs into the membrane structure, along with the precise selection of functional groups, was essential in improving the physical and chemical properties of the membranes. These structural modifications not only enhanced power and current densities, but also contributed to the improved operational efficiency and long-term stability of direct methanol fuel cells (DMFCs) under various working conditions.
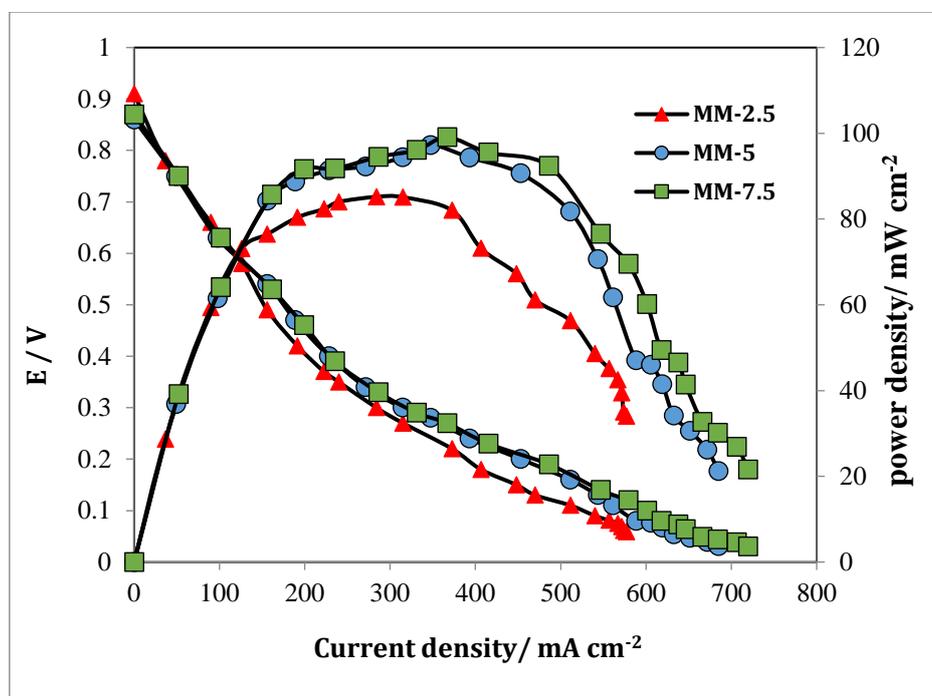

Figure 5. Current density-potential (I-V) and power density curves of the DMFC assembled with different prepared membranes at 80 °C

Conclusion

In this study, sulfonated polystyrene-based nanocomposite membranes incorporating different loadings of MIL-101(Cr) (2.5, 5, and 7.5 wt%) were successfully fabricated via a solution-casting method and systematically evaluated for direct methanol fuel cell (DMFC) and proton exchange membrane fuel cell (PEMFC)

applications. The incorporation of MIL-101(Cr) had a pronounced and quantifiable impact on the physicochemical, electrochemical, and single-cell performance of the membranes. The results demonstrated that increasing the MIL-101(Cr) content significantly enhanced water uptake from 38.2% for MM-2.5 to 48.6% for MM-7.5, while maintaining controlled swelling behavior. The ion exchange capacity reached a maximum value of

0.95 meq g^{-1}, confirming the effective contribution of both sulfonic acid groups in SPS and amine-functionalized sites in MIL-101(Cr) to proton-exchange capability. Proton conductivity showed a clear dependence on MOF loading and operating conditions, achieving a maximum value of 0.0914 S cm^{-1} at 80 °C and 60% relative humidity for the MM-7.5 membrane, which represents a substantial improvement compared to the MOF-free SPS@PE membrane. Despite the increased hydrophilicity, methanol permeability remained in the order of 10^{-7} cm^2 s^{-1} for all composite membranes, indicating that the incorporation of MIL-101(Cr) did not lead to excessive methanol crossover. Consequently, the selectivity factor (σ/P) was significantly enhanced, reaching 5.76×10^4 S·s·cm^{-3} for MM-7.5, highlighting the well-balanced trade-off between proton transport and fuel barrier properties. In addition, all composite membranes exhibited excellent oxidative stability, retaining more than 97% of their initial weight after exposure to Fenton's reagent at 80 °C, confirming their robustness under harsh oxidative conditions. Single-cell DMFC tests further validated the advantages of MIL-101(Cr) incorporation, with the MM-5 and MM-7.5 membranes delivering a maximum power density of approximately 99.05 mW cm^{-2} and a peak current density of up to 719.57 mA cm^{-2} at 80 °C. These improvements are attributed to the synergistic effects of enhanced hydrogen-bonding networks, increased water retention, and additional proton-conducting pathways provided by the MOF structure. Overall, this work demonstrates that MIL-101(Cr) is an effective multifunctional nanofiller for SPS-based membranes, enabling simultaneous enhancement of proton conductivity, selectivity, oxidative stability, and single-cell performance. The results confirm the strong potential of these nanocomposite membranes for application in next-generation DMFCs and PEMFCs. Future studies will focus on long-term durability and further optimization of the MOF–polymer interface to maximize performance under prolonged operating conditions.

Acknowledgments

Disclosure Statement

No potential conflict of interest was reported by the authors in this work.

ORCID

Valiollah Mandanipour:
https://orcid.org/0000-0001-5249-3423
Gholamreza Karimipour:
https://orcid.org/0000-0001-8097-5235
Morteza Montazerozohori:
https://orcid.org/0000-0001-8897-4683
Masoumeh Salehi:
https://orcid.org/0000-0003-3805-7072

References

[1] Olbrich, W., Kadyk, T., Sauter, U., Eikerling, M., Gostick, J. Structure and conductivity of ionomer in PEM fuel cell catalyst layers: a model-based analysis. *Scientific Reports*, **2023**, 13(1), 14127.

[2] Tellez-Cruz, M.M., Escorihuela, J., Solorza-Feria, O., Compañ, V. Proton exchange membrane fuel cells (PEMFCs): Advances and challenges. *Polymers*, **2021**, 13(18), 3064.

[3] Tai, M.H., Thiam, H.S., Tee, S.F., Lim, Y.S., Saw, L.H., Lai, S.O. Self-healing sulfonated poly (ether ether ketone)-based polymer electrolyte membrane for direct methanol fuel cells: Effect of solvent content. Polymers, **2023**, 15(24), 4641.

[4] Palanisamy, G., Thangarasu, S., Oh, T.H. Effect of sulfonated inorganic additives incorporated hybrid composite polymer membranes on enhancing the performance of microbial fuel cells. *Polymers*, **2023**, 15(5), 1294.

[5] Mulijani, S., Dahlan, K., Wulanawati, A. Sulfonated polystyrene copolymer: synthesis, characterization and its application of membrane for direct methanol fuel cell (DMFC). *International Journal of*

Materials, Mechanics and Manufacturing, **2014**, 2(1), 36-40.

[6] Pulungan, A.N. Polymer electrolyte membrane fuel cell from sulfonated polystyrene and maleated natural rubber blend. *Rasayan Journal of Chemistry* , **2020**, 13(2), 1112-1123.

[7] Segale, M., Seadira, T., Sigwadi, R., Mokrani, T., Summers, G. A new frontier towards development of efficient SPEEK polymer membranes for PEM fuel cells applications: A review. *Materials Advances*, **2024**, 5, 7979-8006.

[8] Mandanipour, V., Sadeghi, M.M.R., Berenji, A.R. Decolorization of methylene blue from an aqueous solution using MIL-53 (Al)-(NH$_2$) @ pani absorbent. *Asian Journal of Green Chemistry*, **2025**, 9(1) 83-100.

[9] Namvar-Mahboub, M., Mandanipour, V. and Ahvaraki, M. MOF-incorporated PVDF adsorptive membrane for dye removal from aqueous solution. *Emergent Materials*, **2025**, 8(1), 349-361.

[10] Rambabu, G.D., Bhat, S., Figueiredo, F.M. Carbon nanocomposite membrane electrolytes for direct methanol fuel cells—A concise review. *Nanomaterials*, **2019**, 9(9), 1292.

[11] Ng, W.W., San Thiam, H., Pang, Y.L., Lim, Y.S., Wong, J., Saw, L.H. Self-sustainable, self-healable sulfonated graphene oxide incorporated nafion/poly (vinyl alcohol) proton exchange membrane for direct methanol fuel cell applications. *Journal of Environmental Chemical Engineering*, **2023**, 11(6), 111151.

[12] Salim, E., Afrizal, A., Zilfadli, Z. Synthesis of Polystyrene Sulfonate and Its Characterization as a Polymer Electrolyte Membrane. *Akta Kimia Indonesia*, **2021**, 6(2), 153-161.

[13] Al-Sabagh, A.M., Moustafa, Y.M., Hamdy, A., Killa, H.M., Ghanem, R.T.M., Morsi, R.E. Preparation and characterization of sulfonated polystyrene/magnetite nanocomposites for organic dye adsorption. *Egyptian Journal of Petroleum*, **2018**, 27(3), 403-413.

[14] Dewi, C., Rahmawati, F., Pramono, E. Synthesis of sulfonated polystyrene from styrofoam waste as manufacturing material polymer electrolyte. In *ITB Graduate School Conference*, **2022**, 2(1) 311-320.

[15] Mandanipour, V., Salehi, M., Karimipour, G., Vakili Azghandi, M., Berenji, A.R. Investigation of MIL-53 (Fe)-(COOH)$_2$ as a filler in sulfonated polystyrene/polyethylene membrane for application in direct methanol fuel cell. *Iranian Journal of Chemistry and Chemical Engineering*, **2023**, 42(9), 2875-2885.

[16] Mandanipour, V., Karimipour, G., Montazerozohoori, M., Salehi, M. Enhanced performance of MIL-100(Cr)-COOH incorporated sulfonated polystyrene@Polyethylene membranes for direct methanol fuel cells. *Journal of applied organometallic chemistry,* **2026**, 6(2), 288-303.

[17] Li, J.R., Sculley, J., Zhou, H.C. Metal–organic frameworks for separations. Chemical reviews, **2012**, 112(2), 869-932.

[18] Zhao, Z., Nie, J., Huang, H., He, F., Wang, K., Yang, P. Experimental Study on the Adsorption Performance of Metal–Organic Framework MIL-101 (Cr) for Indoor Toluene. *Buildings*, **2025**, 15(14), 2506.